Final Summary - Kogularamanan Suntharalingam

Phenanthriplatin and $OsNphenCl_3$ Nanoparticle Project

Introduction

Platinum based chemotherapy is the frontline treatment for many systemic malignancies.[1,2] Platinum drugs such as cisplatin [Platinol®], carboplatin [Paraplatin®] and oxaliplatin [Eloxatin®] form bi-functional cross-links with DNA. These adducts prevent DNA synthesis/replication and ultimately lead to tumor cell death.[3-7] Although these platinum drugs are extremely effective against solid tumours, ca. 50% of which are treated with platinum drugs, many cancers display intrinsic, acquired and cross-resistance.[8-10] It is therefore of great interest to develop novel anti-cancer drugs that are active against platinum-resistant tumors and at the same time develop suitable drug delivery systems for transporting these new constructs to the desired site(s) of action.

To address these goals, we have recently focused our efforts on positively charged mono-functional platinum agents[11] and nanoparticle devices.[12-15] In the process we discovered phenanthriplatin, a mono-functional agent that displays better cancer cell toxicity, cellular uptake, DNA binding and transcription inhibition properties, and a unique cancer cell-killing profile than any other platinum agent reported to date.[11] Using our prior experience in coupling platinum-based chemotherapy with nanotechnology for drug delivery, we encapsulated phenanthriplatin in FDA-approved amphiphilic polymers, poly(D,L-lactic-co-glycolic acid)-b-poly(ethylene glycol) (PLGA-b-PEG) nanoparticles (NPs) using the double emulsion technique, and successfully delivered them to tumours in vivo. Encouragingly, our preliminary data indicated that the nanoparticle formulation is able to halt tumour growth. The encapsulated phenanthriplatin nanoparticles, however, had several disadvantageous properties, such as poor loading (ca. 1%) and large size (170 nm diameter). Moreover, recent studies conducted in collaboration with the Hemann group (Koch Institute), where an RNAi-based approach was used to determine the global transcriptional changes induced upon phenanthriplatin and nanoparticle treatment, revealed that the free complex and the nanoparticle yielded completely different cellular response profiles. The present study sought to devise phenanthriplatin nanoparticles with; (1) higher loading, (2) smaller diameter size (50-100 nm) and (3) unaltered cellular response profiles compared to the free phenanthriplatin complex.

Recently we reported the anti-proliferation properties for a series of osmium (VI) nitrido complexes.[16] The 1,10-phenanthroline-bearing complex, $OsNphenCl_3$ displayed 8-fold higher potency for cancer cells over normal fibroblast cells. In order to further reduce toxicity towards normal cells and develop delivery systems that can transport this promising class of compounds to tumours in vivo, we prepared $OsNphenCl_3$ encapsulated PLGA-b-PEG nanoparticles. To the best of our knowledge these are the first osmium containing polymeric nanoparticles developed for cancer therapy.

Experimental Details

Materials. $[Pt(NH_3)_2(phenanthridine)Cl][NO_3]$ and $OsNphenCl_3$ were prepared as previously reported.[11,16]

Nanoparticle Encapsulation. A 0.5 mL DMF solution containing 10 mg of *m*PEG-PLGA (5000:20000 Da, 1:1 LA:GA) and an amount of phenanthriplatin or $OsNphenCl_3$ to give the desired feed, defined as (mg of phenanthriplatin or $OsNphenCl_3$ /mg of polymer) × 100, was prepared. This solution was added in a dropwise manner over the course of 10 min to 5 mL of rapidly stirring ddH_2O water. The DMF solutions were added by a mechanical pipet, and the nanoprecipitations were carried out in 20 mL glass scintillation vials. The water was stirred magnetically using a 0.5 cm stir bar at approximately 800 rpm. After addition of the DMF solution, the water acquired a milky blue (phenanthriplatin) or purple ($OsNphenCl_3$) coloration owing to Tyndall scattering of the nanoparticles that formed. At higher loadings, some macroscopic precipitation was also observed. ddH_2O water then added along the edge of the vial to bring the final volume to 10 mL and the final. This suspension of nanoparticles was stirred for an additional 20 min and then loaded into an Amicon Centrifugal Filtration Device (100 kDa MWCO regenerated cellulose membrane). The loaded device was centrifuged at 1500g for 20 min, concentrating the nanoparticle suspension to approximately 1 mL. This concentrated material was suspended in an additional 10 mL of fresh ddH_2O water and centrifuged again under identical conditions. Each sample was washed three times in this manner. The final concentrated suspension was diluted to 1.0 mL with Milli-Q water for use in further experiments. All nanoprecipitations were carried out in duplicates.

Nanoparticle Loading. The metric used to evaluate encapsulation efficacy was the concentration of platinum or osmium present in the final 1.0 mL colloidal suspension. This concentration was determined by electrothermal atomic absorption spectroscopy (AAS) using a Perkin-Elmer AAnalyst 600 spectrometer outfitted with a transverse heated graphite atomizer. Platinum and osmium absorption were measured at 265.9 nm and 290.9 nm respectively, and a Zeeman background absorption correction was applied. Samples were prepared by diluting nanoparticle suspensions with Milli-Q water until the platinum or osmium concentration fell within the linear calibration range (50−200 μg of Pt/L and 500-2500 μg of Os/L). All AAS measurements were carried out in triplicate and averaged.

Nanoparticle Size. Aqueous solutions of the nanoparticle formulations were diluted to concentrations within the linear dynamic range (50-200 μg Pt/L or μg Os/L) of the spectrometer using ddH_2O. The nanoparticle size (diameter in nm) was recorded using a DynaPro NanoStar Light Scatterer instrument. The data was processed and analysed using the DYNAMICS software package.

Cell Lines and Cell Culture Conditions. A549 lung adenocarcinoma and MRC-5 normal human fetal lung fibroblast cell lines were maintained in Dulbecco's Modified Eagle's Medium

(DMEM-low glucose) supplemented with 10% fetal bovine serum and 1% penicillin/streptomycin. The cells were grown at 310 K in a humidified atmosphere containing 5% CO2.

Cytotoxicity MTT assay. The colourimetric MTT assay was used to determine the toxicity of $[Pt(NH_3)_2(phenanthridine)Cl][BPh_4]$, **Ptphen NP**, **Os NP**. Cells (2×10^3) were seeded in each well of a 96-well plate. After incubating the cells overnight, various concentrations of platinum as determined by GF-AAS (0.3-100 μM) were added and incubated for 72 h (total volume 200 μL). **Ptphen NP** and **Os NP** were prepared as 1-2 mM solutions in ddH_2O and diluted using media. $Pt(NH_3)_2(phenanthridine)Cl][BPh_4]$ was prepared as 10 mM solution in DMSO and diluted using media. The final concentration of DMSO in each well was 0.5% and this amount was present in the untreated control as well. Cisplatin was prepared as a 5 mM solution in PBS and diluted further using media. After 72 h, the medium was removed, 200 μL of a 0.4 mg/mL solution of MTT in DMEM was added, and the plate was incubated for an additional 1-2 h. The DMEM/MTT mixture was aspirated and 200 μL of DMSO was added to dissolve the resulting purple formazan crystals. The absorbance of the solution wells was read at 550 nm. Absorbance values were normalized to DMSO-containing control wells and plotted as concentration of test compound versus % cell viability. IC_{50} values were interpolated from the resulting dose dependent curves. The reported IC_{50} values are the average from at three independent experiments, each of which consisted of six replicates per concentration level.

Cellular Uptake. To measure the cellular uptake of $[Pt(NH_3)_2(phenanthridine)Cl][BPh_4]$, **Ptphen NP**, $OsNphenCl_3$, and **Os NP** ca. 2 million A549 cells were treated with 5 μM of $[Pt(NH_3)_2(phenanthridine)Cl][BPh_4]$, **Ptphen NP**, $OsNphenCl_3$, and **Os NP** and incubated at 37°C, 4°C, and in the presence of endocytosis inhibitors, NH_4Cl (50 mM) and chloroquine (100 μM) for 4 h. Then the media was removed, the cells were washed with PBS solution (1 mL × 3), harvested, and centrifuged. The cellular pellet mineralized with 65% HNO_3 and then completely dried at 120 ºC. The solid extracts were re-dissolved in 4% HNO_3 and analysed using graphite furnace atomic absorption spectroscopy (Perkin-Elmer AAnalyst600 GF-AAS). Cellular platinum and osmium levels were expressed as ng of Pt and Os per million cells. Results are presented as the mean of three determinations for each data point.

RNAi Signatures. Compounds were dosed to achieve an LD80-90 in Eμ-Mycp$^{19arf-/-}$ cells by propidium iodide exclusion as determined by FACS after 48 h incubation. GFP enrichment/depletion was then determined by FACS at 72 h. Linkage ratios (LR) and p-values were generated as described previously.[17-19] All FACS was conducted using a FACScan (BD Biosciences).

GFP Competition assays. Eμ-Mycp$^{19arf-/-}$ lymphoma or p185+ BCR-Abl$^{p19arf-/-}$ leukemia cells were infected with GFP-tagged shRNAs such that 15-25% of the population were GFP positive. An eighth of a million cells in 250 μL B-cell media (BCM) were then seeded into 24-well plates. For wells that would remain untreated as a control, only 1/16th of a million cells were seeded.

Next, 250 μL of media containing the active agent was added to the cells. After 24 h, 300 μL of cells from untreated wells are removed and replaced by 300 μL fresh BCM. All wells then received 500 μL BCM before being placed by in the incubator for another 24 h. At 48 h, cells transduced with the control vector, MLS, were checked for viability via FACS on a FACScan (BD Biosciences) using propidium iodide as a live/dead marker. Untreated wells then had 700 μL of cells removed and replaced with 700 μL fresh media followed by a further 1 mL of fresh media. Wells for which the compound had killed 80-90% of cells (LD80-90) were then diluted further by adding 1 mL of BCM. Finally, at 72 h, all wells for which an LD80-90 was achieved, as well as the untreated samples, were analysed via FACS to determine GFP% enrichment.

Results and Discussion

Nanoparticle Formulation for Ptphen NP. The double emulsion technique afforded phenanthriplatin encapsulated nanoparticles with 0.5-1 % loading (mg of phenanthriplatin encapsulated/ mg of polymer). To improve loading and hence create more biologically useful nanoparticle constructs, we modified phenanthriplatin such that the nanoprecipitation (single emulsion) technique could be employed. Phenanthriplatin as the nitrate salt, $[Pt(NH_3)_2(phenanthridine)Cl]NO_3$ was not conducive to nanoprecipitation due to its hydrophilic nature. Therefore the hydrophobicity of phenanthriplatin was increased by exchanging the counter-anion for tetraphenylborate (carried out by **Timothy C. Johnstone**). Structural changes to the phenanthriplatin cation were avoided to preserve the biologically activity of the compound.

With the hydrophobic phenanthriplatin derivative, $[Pt(NH_3)_2(phenanthridine)Cl][BPh_4]$ in hand, phenanthriplatin encapsulated nanoparticles were prepared using the nanoprecipitation technique. The specific experimental encapsulation method is given in the Experimental section. Briefly, a DMF solution containing the *m*PEG-PLGA polymer and the tetraphenylborate phenanthriplatin complex were added in a dropwise manner to rapidly stirring water (10 times excess). As a DMF droplet comes into contact with water, the organic solvent instantaneously disperses into the aqueous phase. This process initiated the self-assembly of the polymer into a nanoparticle micelle with a hydrophilic exterior and hydrophobic interior. The hydrophobic phenanthriplatin complex became trapped in the hydrophobic core of the nanoparticle.

Phenanthriplatin encapsulated nanoparticles (**Ptphen NP**) were prepared using a range of feeds. Feed refers to percentage (w/w) phenanthriplatin to polymer. The amount of phenanthriplatin encapsulated was gauged by measuring the platinum content of the nanoparticle using graphite force atomic absorption spectroscopy. As the feed was increased from 5% to 10%, the amount of phenanthriplatin encapsulated increased as quantified by the loading and encapsulation efficiency (Figure 1). Loading is the percent (w/w) of phenanthriplatin encapsulated with respect to polymer used and encapsulation efficiency is the percent (w/w) of phenanthriplatin encapsulated

with respect to phenanthriplatin used. Upon increasing the feed beyond 10%, the macroscopic precipitates began to form during the nanoprecipitation process. The formation of large precipitates severely hampered the encapsulation process and thus the loading and encapsulation efficiency decreased beyond 15%. A maximum loading and encapsulation efficiency of 3.2% and 15.8% respectively, were obtained when the feed was 15%. These values were 3-4 fold higher than those obtained for phenanthriplatin encapsulated nanoparticles prepared using the double emulsion method.

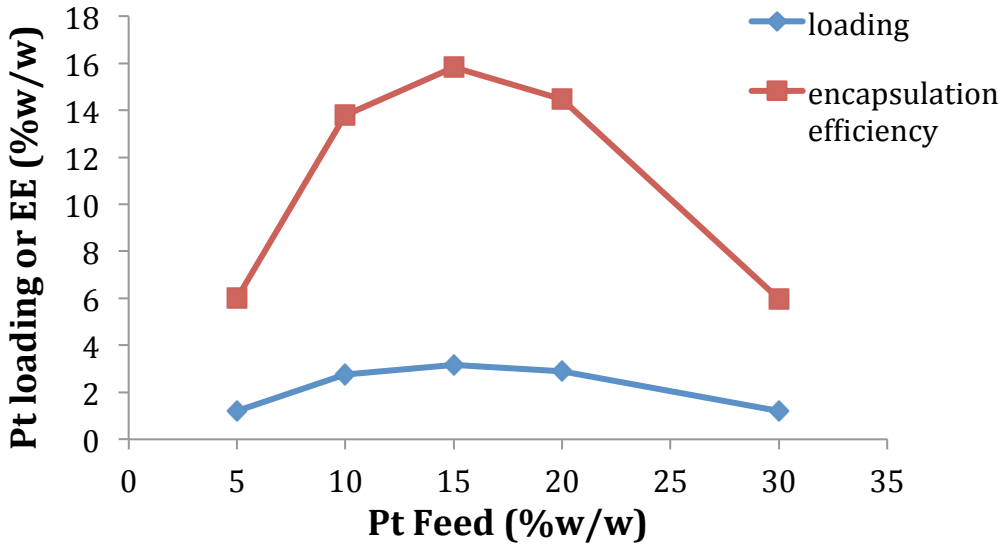

Figure 1. The effect of feed variation on loading and encapsulation efficiency of $[Pt(NH_3)_2(phenanthridine)Cl][BPh_4]$ encapsulated nanoparticles, **Ptphen NP**.

The size of each nanoparticle formulation was probed by dynamic light scattering. The size was determined by taking the radius reading at the maximum intensity of fluctuation from the dynamic light scattering intensity distribution trace. As the feed was increased from 5% to 30%, the diameter of the nanoparticle increased slightly (Table 1); suggesting that feed was not a major determinant of nanoparticle size. The nanoparticle diameter varied from 130 – 150 nm, an ideal size to exploit the enhanced permeability and retention (EPR) effect. Taking into account the loading, encapsulation efficiency, and size, the nanoparticles produced when using a 15% feed were deemed the most suitable for biological studies.

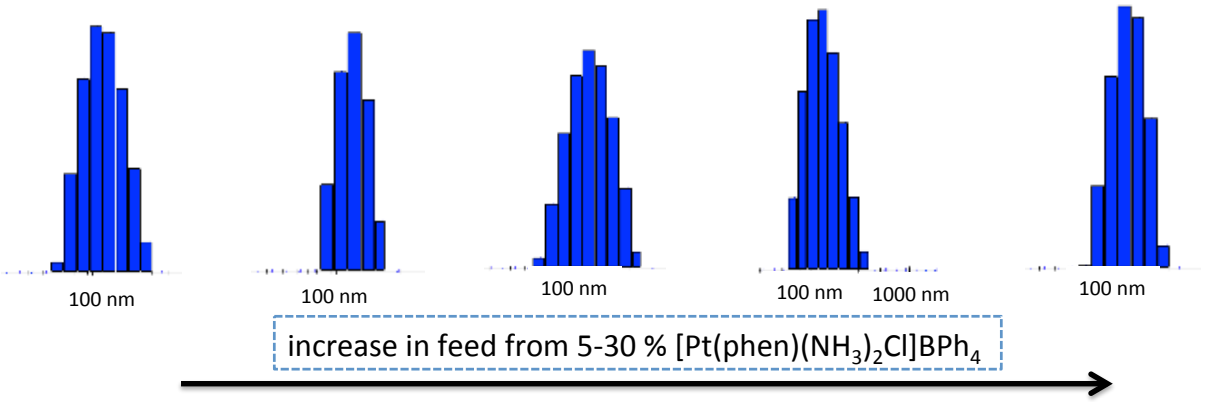

Figure 2. Dynamic light scattering intensity distribution trace obtained for **Ptphen NP** formulated with $[Pt(NH_3)_2(phenanthridine)Cl][BPh_4]$ different feeds (5-30%).

Table 1. The radius (in nm) of **Ptphen NP** as determined by dynamic light scattering analysis. The feed (%w/w) was not a major determinant of nanoparticle size.

Feed (%w/w)	Radius (nm)
5	65.326
10	67.78
15	75.575
20	73.017
30	75.371

Nanoparticle Formulation for Os NP. Owing to the large phenanthroline ligand and its neutral charge, $OsNphenCl_3$ is intrinsically hydrophobic. Indeed the LogP of $OsNphenCl_3$, as determined by the shake-flask method, is 1.26. Therefore $OsNphenCl_3$ was used without modification to generate osmium-containing *m*PEG-PLGA polymeric nanoparticles, **Os NP**. The same procedure as that described above for **Ptphen NP** was used, however, the feed was varied from 5% to 60%. The loading and encapsulation efficiency were calculated for each formulation by measuring the osmium content of the nanoparticle using graphite force atomic absorption spectroscopy. The change in loading and encapsulation efficiency as function of feed is illustrated in Figure 3. A maximum loading and encapsulation efficiency of 1.1% and 5.6% respectively, were obtained when the feed was 30%.

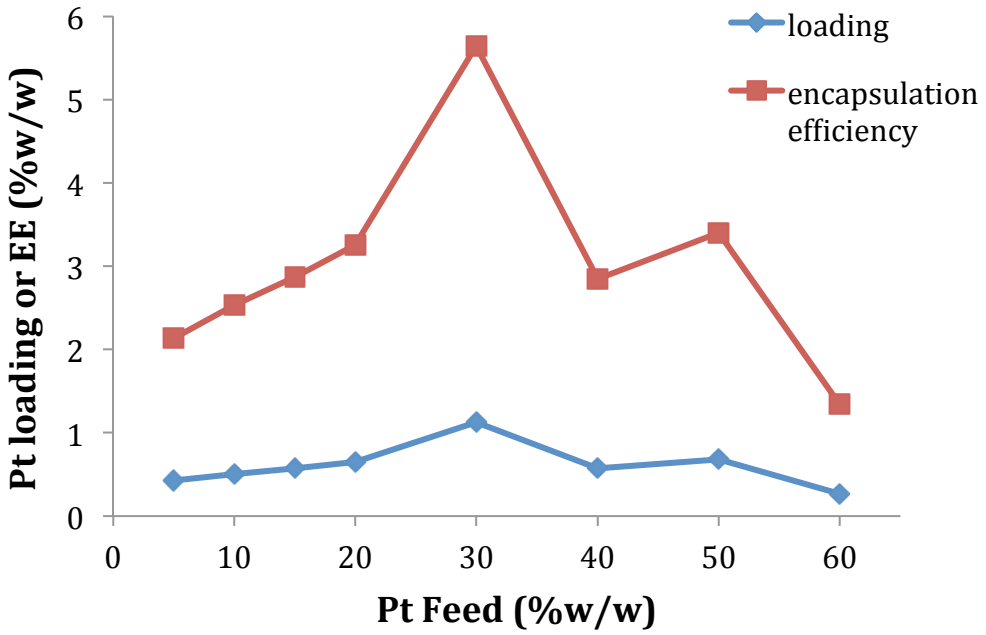

Figure 3. The effect of feed variation on loading and encapsulation efficiency of $OsNphenCl_3$ encapsulated nanoparticles, **Os NP**.

The size of the $OsNphenCl_3$ encapsulated nanoparticles, **Os NP** was dependent on feed. As the feed was increased from 5% to 30% the diameter increased by 36 nm. Notably the nanoparticle size remained fairly constant between 30% and 60% feed. Taking into account the loading, encapsulation efficiency, and size, the nanoparticles produced when using a 30% feed were deemed the most suitable for in vitro studies.

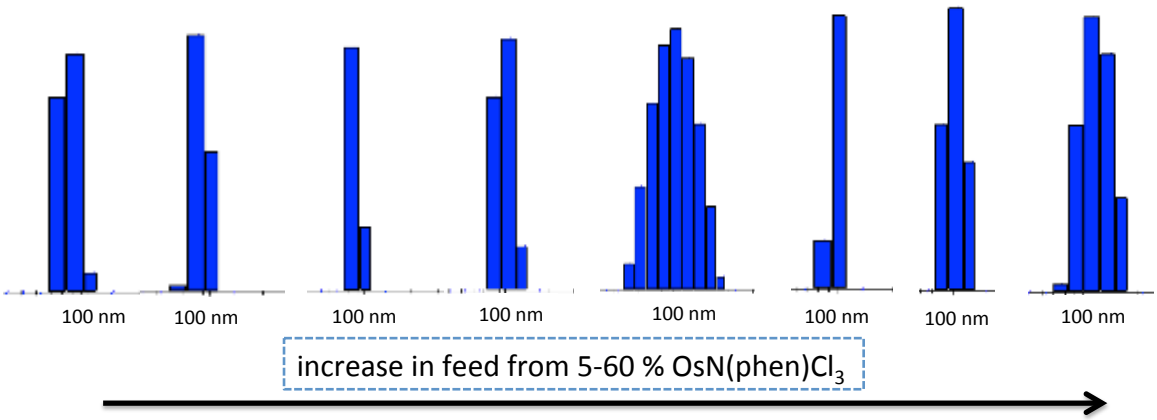

Figure 4. Dynamic light scattering intensity distribution trace obtained for **Os NP** formulated with different $OsNphenCl_3$feeds (5-30%).

Table 2. The radius (in nm) of **Os NP** as determined by dynamic light scattering analysis. The feed (%w/w) in case is a determinant of nanoparticle size.

Feed (%)	Radius (nm)
5	**38.757**
10	**45.887**
15	**44.444**
20	**50.235**
30	**56.616**
40	**51.666**
50	**53.335**
60	**59.029**

Biological Studies. To establish the therapeutic potential of the $[Pt(NH_3)_2(phenanthridine)Cl][BPh_4]$ and $OsNphenCl_3$ encapsulated nanoparticles, **Ptphen NP** and **Os NP** their cytotoxicity against lung carcinoma (A549) and lung fibroblast (MRC-5) cells were determined using the colorimetric MTT assay. The free platinum and osmium complexes were also tested as controls. The IC_{50} values (concentration required to induce 50% inhibition) were derived from dose-response curves and are summarised in Figure 5 and Table 3. **Ptphen NP** displayed sub-micromolar toxicity against A549 cells, however, selectivity over normal MRC-5 cells was poor (2.5-fold). A similar trend was also observed for the free $[Pt(NH_3)_2(phenanthridine)Cl][BPh_4]$ complex. Remarkably, **Os NP** exhibits no toxicity towards A549 or MRC-5 cells, in contrast to the free complex, $OsNphenCl_3$, which displayed micromolar toxicity. The poor activity of **Os NP** could be explained by entrapment inside the cell membrane or early endosomal vesicles.

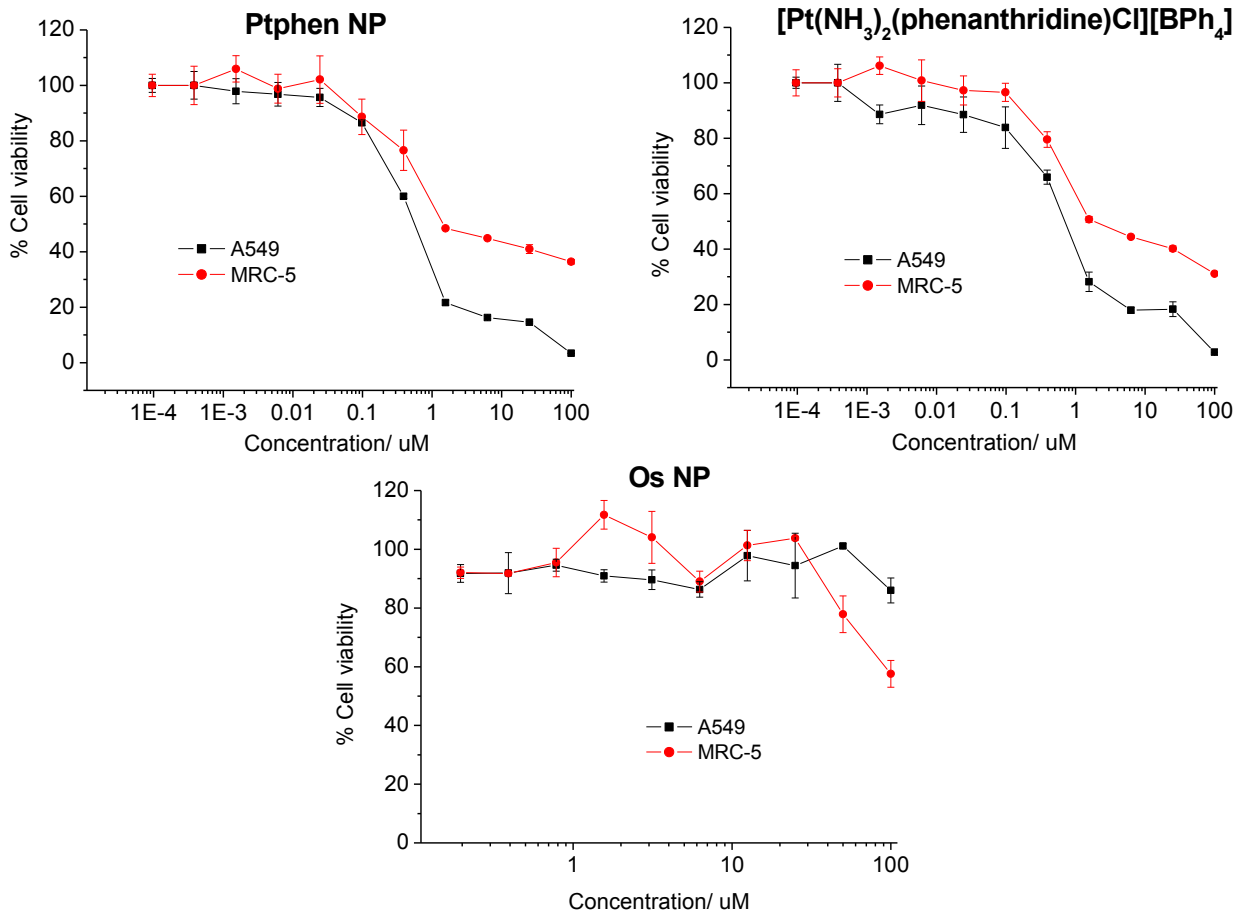

Figure 5. Representative lung carcinoma (A549) and lung fibroblast (MRC-5) MTT Dose-Response Curves

Table 3. IC_{50} values (in μM) of **Ptphen NP**, **Os NP**, $[Pt(NH_3)_2(phenanthridine)Cl][BPh_4]$ and $OsNphenCl_3$ against lung carcinoma (A549) and lung fibroblast (MRC-5) cells. The values reported are an average of three independent determinations. [a] IC_{50} values taken from Ref. 16.

	A549 (lung carcinoma)	MRC-5 (lung fibroblast)
Ptphen NP	0.56 ± 0.01	1.45 ± 0.15
$[Pt(NH_3)_2(phenanthridine)Cl][BPh_4]$	0.63 ± 0.15	2.28 ± 0.38
Os NP	> 100	> 100
$OsNphenCl_3$	7.86 ± 1.41 [a]	16.59 ± 3.61 [a]

To determine if the nanoparticle constructs could enter cells, cellular uptake studies were performed. The free platinum and osmium complexes were also analysed for comparison. Lung carcinoma A549 cells were incubated with a sub-lethal dose (5 μM) of **Ptphen NP**, **Os NP**,

[$Pt(NH_3)_2$(phenanthridine)Cl][BPh_4] and $OsNphenCl_3$ for 4 h at 37°C. The cells were washed, harvested, and the platinum or osmium content was measured by GF-AAS.

Ptphen NP was readily taken up by cells at 37°C, 2.5-fold higher than the free compound under the same conditions. To determine the temperature dependence of nanoparticle uptake, and thereby gain insight into whether the process is active or passive; the experiment was conducted at 4°C (Fig. 6). When cells were incubated with **Ptphen NP** at 4°C, a 6-fold decrease in platinum uptake was observed, indicative active uptake. Polymeric nanoparticles, such as those used in this study are prone to undergo energy- and temperature-dependent endocytic uptake. To determine if **Ptphen NP** undergoes endocytosis, cells were co-incubated with endocytosis inhibitors, namely ammonium chloride and chloroquine. Under these conditions, a statically significant decrease in uptake was observed, suggesting that **Ptphen NP** enters cells via the endocytic pathway. [$Pt(NH_3)_2$(phenanthridine)Cl][BPh_4] uptake was relatively unaffected by ammonium chloride or chloroquine (lysosomotropic agents) indicative of a non-endocytic, passive mechanism of uptake.

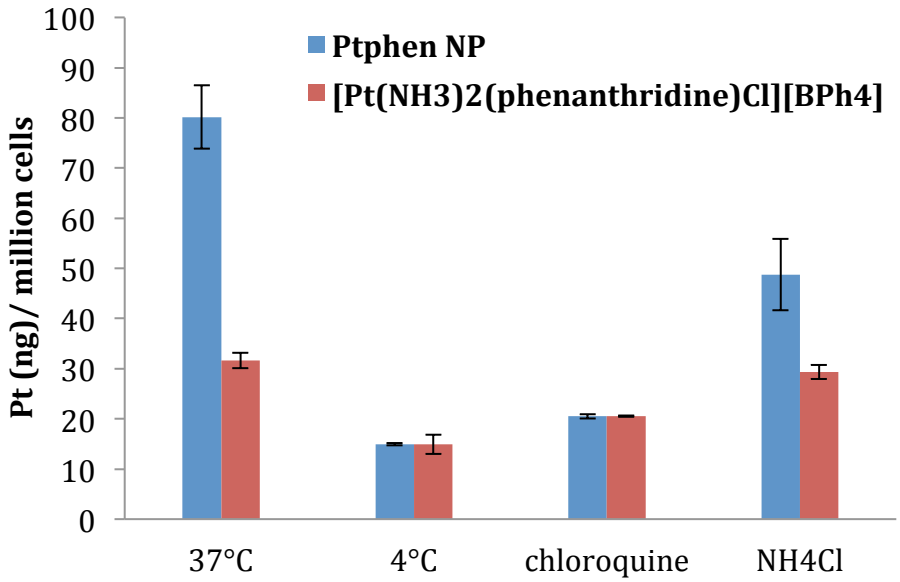

Figure 6. Platinum content (ng per million cells) isolated from A549 cells treated with **Ptphen NP** and [$Pt(NH_3)_2$(phenanthridine)Cl][BPh_4] under various conditions (5 µM for 4 h).

Os NP and the corresponding free complex, $OsNphenCl_3$ were taken up equally by cells at 37°C (Fig. 7). **Os NP** accumulation is comparable to **Ptphen NP**. **Os NP** displays reduced uptake at 4°C, and in the presence of ammonium chloride or chloroquine, indicative of endocytic uptake. In light of the cellular uptake and cytotoxicity data, it is evident that **Os NP** is able to enter cells without exhibiting potency. This could be due to entrapment inside the endosomal vesicles, alternatively the encapsulated $OsNphenCl_3$ may become inactivated in the mildly acidic endosomal environment (pH 6.0-6.5). Free $OsNphenCl_3$ uptake is not affected by temperature, ammonium chloride, or chloroquine, symbolic of passive uptake.

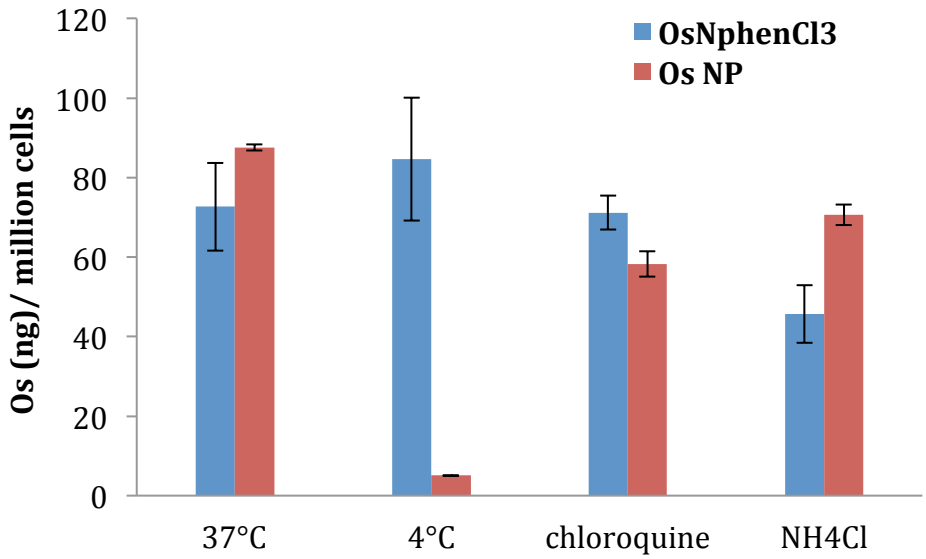

Figure 7. Osmium content (ng per million cells) isolated from A549 cells treated with **Os NP** and $OsNphenCl_3$ under various conditions (5 μM for 4 h).

To characterise the cytotoxic mechanism of action of **Ptphen NP** and $[Pt(NH_3)_2(phenanthridine)Cl][BPh_4]$, a newly developed RNAi-based drug signature assay was used. This was carried out in collaboration with the Hemann group (Koch Institute). The RNAi-based approach uses lymphoma cells partially infected with one of eight distinct short hairpin RNAs (shRNAs). Upon drug treatment, shRNA infected cells will either enrich or deplete depending on the advantage or disadvantage conferred by a given shRNA. The response of these cells evokes signatures, which have been determined for many classes of clinically used cytotoxic agents. The signature derived for a novel compound or nanoparticle formulation is compared to those of a reference set of drugs using a probabilistic K-nearest-neighbors algorithm to determine whether it belongs to a class in the reference set or a new category that is not represented in the reference set. The **Ptphen NP** and $[Pt(NH_3)_2(phenanthridine)Cl][BPh_4]$ signatures resembled those obtained for transcription/ translation inhibitors such as rapamycin and puromycin (Fig. 8). Moreover, unlike nanoparticles generated using the double emulsion technique, which prompted a different cellular response to the parent complex, **Ptphen NP** gave a very similar iRNA signature to the free complex, $[Pt(NH_3)_2(phenanthridine)Cl][BPh_4]$.

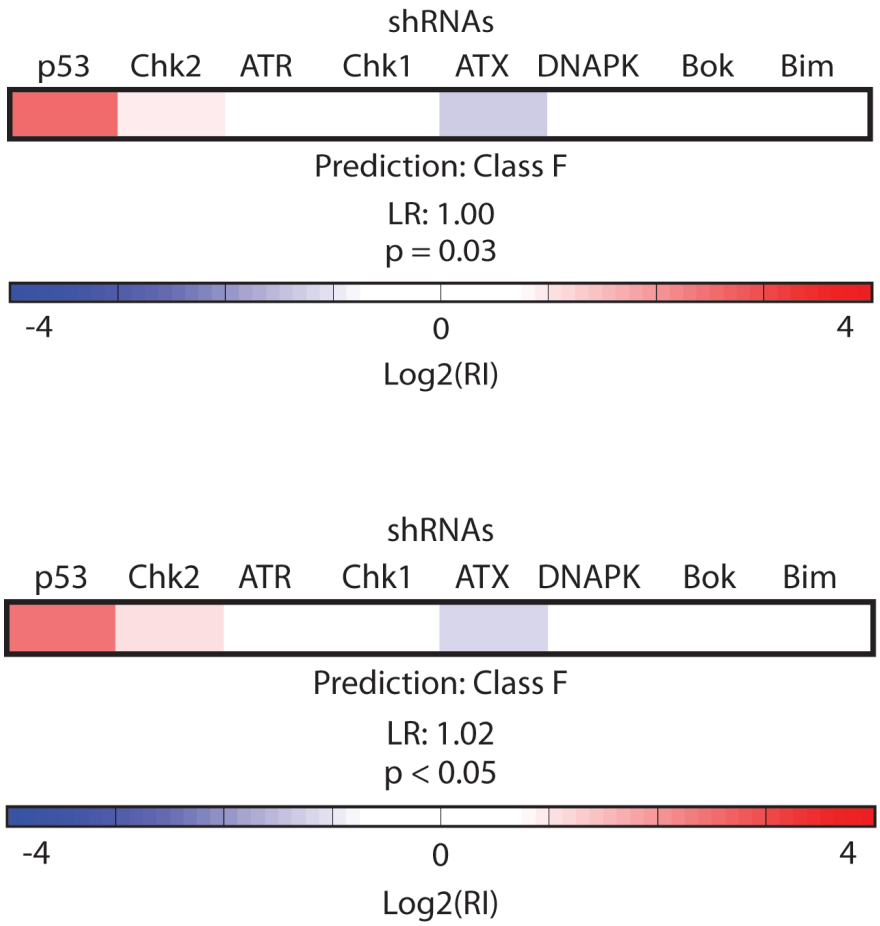

Figure 8. RNAi signatures derived from the treatment of Eμ-Mycp$^{19arf-/-}$ lymphoma cells with (top) **Ptphen NP** and (bottom) $[Pt(NH_3)_2(phenanthridine)Cl][BPh_4]$ at the LD80−90 concentration for each compound.

Conclusion and Future Direction.

A new phenanthriplatin-*m*PEG-PLGA formulation, **Ptphen NP** was prepared by nanoprecipitation. **Ptphen NP** displayed superior physical properties, such as higher loading and smaller size, compared to previously prepared phenanthriplatin nanoparticles formulations. **Ptphen NP** exhibited impressive in vitro toxicity toward lung carcinoma A549 cells, however, selectivity over normal lung fibroblast MRC-5 cells was poor (2.5 fold). A similar trend was also observed for the free complex, $[Pt(NH_3)_2(phenanthridine)Cl][BPh_4]$. The new nanoparticle formulation delivered 6-fold higher platinum into cells than the free complex. The cellular uptake pathway was characterised as endocytosis, a common uptake process for polymeric nanomaterial. Importantly, **Ptphen NP** produced a similar iRNA cellular mechanism signature to $[Pt(NH_3)_2(phenanthridine)Cl][BPh_4]$, suggesting a closely related cytotoxic mechanism of action.

The fact the **Ptphen NP** construct does not change the cellular properties of the payload, unlike previous formulations, augers well for in vivo application.

$OsNphenCl_3$ encapsulated nanoparticles, **Os NP** with reasonable loading and biological appropriate size were also prepared using the nanoprecipitation method. **Os NP** readily penetrates cells, however, potency towards cancer cells was very poor (IC_{50} > 100 μM). It is likely that **Os NP** becomes entrapped or deactivated in the early endosomal vesicles. To overcome this problem, synthetic peptides (e.g. KALA, influenza HA-2, JTS-1) that undergo structural changes in the acidic endosomal environment will be incorporated into the nanoparticle formulation. These changes are expected to disrupt the vesicle membrane and thus allow release of the nanoparticles and payload.

Reference.

(1) Fricker, S. P. *Dalton Trans.* **2007**, 4903.
(2) Kelland, L. *Nat. Rev. Cancer* **2007**, *7*, 573.
(3) Jung, Y.; Lippard, S. J. *Chem. Rev.* **2007**, *107*, 1387.
(4) Lippard, S. J. *Science* **1982**, *218*, 1075.
(5) Lippert, B. *Cisplatin : chemistry and biochemistry of a leading anticancer drug*; Verlag Helvetica Chimica Acta ; Wiley-VCH: Zürich Weinheim ; New York, 1999.
(6) Todd, R. C.; Lippard, S. J. *Metallomics* **2009**, *1*, 280.
(7) Wang, D.; Lippard, S. J. *Nat. Rev. Drug Discovery* **2005**, *4*, 307.
(8) Brabec, V.; Kasparkova, J. *Drug Resist. Updates* **2005**, *8*, 131.
(9) McWhinney, S. R.; Goldberg, R. M.; McLeod, H. L. *Mol. Cancer Ther.* **2009**, *8*, 10.
(10) Siddik, Z. H. *Oncogene* **2003**, *22*, 7265.
(11) Park, G. Y.; Wilson, J. J.; Song, Y.; Lippard, S. J. *Proc. Natl. Acad. Sci.* **2012**, *109*, 11987.
(12) Feazell, R. P.; Nakayama-Ratchford, N.; Dai, H.; Lippard, S. J. *J Am Chem Soc* **2007**, *129*, 8438.
(13) Dhar, S.; Liu, Z.; Thomale, J.; Dai, H.; Lippard, S. J. *J Am Chem Soc* **2008**, *130*, 11467.
(14) Dhar, S.; Gu, F. X.; Langer, R.; Farokhzad, O. C.; Lippard, S. J. *Proc Natl Acad Sci U S A* **2008**, *105*, 17356.
(15) Dhar, S.; Daniel, W. L.; Giljohann, D. A.; Mirkin, C. A.; Lippard, S. J. *J Am Chem Soc* **2009**, *131*, 14652.
(16) Suntharalingam, K.; Johnstone, T. C.; Bruno, P. M.; Lin, W.; Hemann, M. T.; Lippard, S. J. *J. Am. Chem. Soc.* **2013**, *135*, 14060.
(17) Jiang, H.; Pritchard, J. R.; Williams, R. T.; Lauffenburger, D. A.; Hemann, M. T. *Nat. Chem. Biol.* **2011**, *7*, 92.
(18) Pritchard, J. R.; Bruno, P. M.; Gilbert, L. A.; Capron, K. L.; Lauffenburger, D. A.; Hemann, M. T. *Proc. Natl. Acad. Sci.* **2013**, *110*, E170.
(19) Pritchard, J. R.; Bruno, P. M.; Hemann, M. T.; Lauffenburger, D. A. *Mol. BioSyst.* **2013**, *9*, 1604.

Publications while funded by the Misrock Fellowship.

- Suntharalingam K, Wilson JJ, Lin W, Lippard SJ, "A Dual-targeting, p53-Independent, Apoptosis Inducing Platinum(II) Anticancer Complex, [Pt(BDIQQ)]Cl", *Metallomics*, **2014**, 6 (3), 437-43
- Suntharalingam K, Ying S, Lippard SJ, "Conjugation of Vitamin E Analog α-TOS to Pt(IV) Complexes for Dual-Targeting Anticancer Therapy" *Chemical Communications*, **2014**, 50 (19), 2465-8
- Suntharalingam K, Johnstone TC, Bruno PM, Lin W, Hemann MT, Lippard SJ, "Bidentate Ligands on Osmium(VI) Nitrido Complexes Control Intracellular Targeting and Cell Death Pathways" *Journal of the American Chemical Society*, **2013**, 135 (38), 14060-14063
- Song Y, Suntharalingam K, Yeung JS, Royzen M, Lippard SJ, "Synthesis and Characterization of Pt(IV) Fluorescein Conjugates to Investigate Pt(IV) Intracellular Transformations" *Bioconjugate Chemistry*, **2013**, 24(10), 1733-1740

Publications submitted or under preparation.

- Suntharalingam K, Johnstone TC, Bruno PM, Hemann MT, Lippard SJ, "A New Nanoparticle Formulation for Phenantriplatin" in preparation
- Suntharalingam K, Johnstone TC, Page JE, Bruno PM, Lin W, Hemann MT, Lippard SJ, "Rhenium (V)-oxo complexes: A New Class of Anticancer Agents", in preparation